Demonstration of all-optical NOT logic gate at bit rate 20Gbps based on SOA-MI with optimum injection current

Demonstração da porta lógica NOT totalmente óptica a uma taxa de bits de 20Gbps baseada em SOA-MI com corrente de injeção ideal

DOI:10.34117/bjdv7n4-251

Recebimento dos originais: 07/03/2021
Aceitação para publicação: 09/04/2021

Jackson Moreira de Oliveira
Mestre em Engenharia Elétrica pela Universidade Federal do Pará
Instituto Federal de Educação, Ciência e Tecnologia do Pará
Endereço: Fl. 22, Q. Esp., Lt. Esp., N. Marabá, CEP 68508-970, Marabá, PA – BR
E-mail: jackson.oliveira@ifpa.edu.br

Fabio Barros de Sousa
Doutorando em Engenharia Elétrica pela Universidade Federal do Pará
Universidade Federal do Pará, Programa de Pós-Graduação em Engenharia Elétrica
Endereço: Rua Augusto Corrêa, 01, CEP 66075-110, Belém, PA – BR
E-mail: fabiobarros.s85@gmail.com

Hudson Afonso Batista da Silva
Mestre em Engenharia Elétrica pela Universidade Federal do Pará
Instituto Federal de Educação, Ciência e Tecnologia do Pará
Endereço: Fl. 22, Q. Esp., Lt. Esp. – N. Marabá, CEP 68508-970, Marabá, PA – BR
E-mail: Hudson.silva@ifpa.edu.br

Lelis Araujo de Oliveira
Doutorando em Engenharia Elétrica pela Universidade Federal do Pará
Instituto Federal de Educação, Ciência e Tecnologia do Pará
Endereço: Fl. 22, Q. Esp., Lt. Esp. – N. Marabá – Marabá, PA – BR
E-mail: lelis.oliveira@ifpa.edu.br

Jorge Everaldo de Oliveira
Doutor em Engenharia Elétrica pela Universidade Federal do Pará
Faculdade de Licenciatura em Física, Universidade Federal do Sul e Sudeste do Pará
Endereço: Fl. 17, Q. Esp., Lt. Esp. – N. Marabá – Marabá – PA – BR
E-mail: joeveraldo@unifesspa.edu.br

Fiterlinge Martins de Sousa
Doutor em Engenharia Elétrica pela Universidade Federal do Pará
Universidade Federal do Pará, Programa de Pós-Graduação em Engenharia Elétrica
Endereço: R. Augusto Corrêa, 01, CEP 66075-110, Belém – PA – BR
E-mail: fiterlinge@ufpa.br

Fabrício Pinho da Luz
Mestre em Engenharia Elétrica pela Universidade Federal do Pará
Universidade Federal do Pará, Programa de Pós-Graduação em Engenharia Elétrica
Endereço: R. Augusto Corrêa, 01, CEP 66075-110, Belém – PA – BR
E-mail: fabriciopluz@gmail.com

Marcos Benedito Caldas Costa
Professor Doutor no Programa de Pós-Graduação em Engenharia Elétrica da Universidade Federal do Pará
Endereço: R. Augusto Corrêa, 01, CEP 66075-110, Belém – PA – BR
E-mail: marcosta@ufpa.br

RESUMO
Neste trabalho, a propriedade não-linear do amplificador óptico semicondutor (SOA) na modulação de ganho cruzado (XGM) é usada com um interferômetro Michelson (MI) formando uma estrutura SOA-MI para executar a porta lógica NOT a 20Gbps para extrair regras de design simples com um sinal de dados de entrada binária. É demonstrado que a alta taxa de dados pode ser alcançada com uma baixa corrente de injeção específica em SOA, o que leva a um valor baixo no consumo total de energia da porta. Além disso, este trabalho inclui o estudo do efeito da taxa de bits na taxa mínima de erro de bit (BER), e no fator de qualidade máximo (max. Q-factor) baseado no diagrama de olho, para os diferentes valores de dados de entrada e corrente de injeção.

Palavras-chave: Porta lógica NOT, Amplificador óptico semicondutor, Interferômetro de Michelson.

ABSTRACT
In this paper, the non-linear property of semiconductor optical amplifier (SOA) on cross gain modulation (XGM) is used with a Michelson interferometer (MI) forming an SOA-MI structure to perform the NOT logic gate at 20Gbps bit rate to extract simple design rules with one binary input data signals. It is demonstrated that high data rate can be achieved with a low specific injection current in SOA, which leads to a low value on the total power consumption of the gate. In addition, this work includes the study of the effect of the bit rate on the minimum bit error rate (BER), and maximum quality factor (max. Q-factor) based on Eye diagram, for the different values of input data and injection current.

Keywords: NOT logic gate, Semiconductor optical amplifiers, Michelson interferometer.

1 INTRODUCTION

In a globalized world is essential that telecommunication systems are capable of handling traffic and information processing at ultra-fast speeds with high bit rate, and the fiber optics are efficient and robust systems. Semiconductor Optical Amplifiers (SOA) are designed to omit the need of converting the signal from optical to electric and vice versa, guaranteeing high data rates, direct amplification of optical signals and energy efficiency considered in all-optical systems (SINGH, TIWARI and RAJCHANDANI,

2014). Duarte et al. also states that the development of technologies such as fiber optics, lasers and MicroElectroMechanical systems (MEMS), combined with GPS, allowed the use of navigation systems in any application where speed and position information is needed.

The SOAs attractive for all-optical signal processing such as all optical switching and wavelength conversion. Moreover, have advantages in terms of low-power consumption, a small footprint, and homogeneous integration. Unitary NOT function is the simplest Boolean functions which performs a logical inversion of the input data (MALHOTRA, ANAND and RAGHAV). The basic key element of all-optical processing is all-optical logic gates which are used for header recognition, signal regeneration, addressing, data encoding (VINOTHINI; SHANMUGAPRIYA and MARGARAT, 2018). The decrease in amplification gain and carrier density of the semiconductor optical amplifier is caused due to increment in input signal power (ARCHANA; MANOHARI and PRINCE, 2018). Since the carrier density change in SOAs will affect all input signals, a signal at one wavelength can affect the gain of a signal at another wavelength (SON et al., 2007).

The pump signal and the probe signal can operate either in co-propagating or counter-propagating configuration through SOA. When injected in co-propagation mode, an optical band-pass filter must be used at the output of the SOA in order to pass the converted probe signal and block the pump. Wavelength conversion can be induced by injecting a strong signal into an SOA. Due to cross gain modulation (XGM), the stronger signal will force the weaker signal to its modulation. As a result, the CW probe signal is modulated via XGM, causing inverted wavelength conversion (MAZLAN et al., 2014).

Several configurations have already been proposed in the literature using the non-linear effect of XGM in SOA. In this sense, several logic gates have already been realized, among them include: AND, OR, NOR and others with their combinations.

Mukherjee and Maji (2019) designed the NAND all-optical universal logic gate using a hybrid coding technique for representation of binary information states, a mixture of four waves in semiconductor optical amplifier (SOA) as frequency generator and cross polarization rotation effect in semiconductor optical amplifier as a frequency converter. In this sense, the system proposed by them was able to perform ultra-fast and easily integrable operations.

Oliveira et al (2019) proposed a new scheme to realize the universal all-optical NAND logic gate at high speed based on the non-linearity of SOA with MI and an optical

filter, based on cross-gain modulation (XGM). The NAND operation was performed by combining the XOR and NOR logic gates, or by joining the AND gates with NOT. In that they showed that the structure based on SOA-MI is viable for the transmission rate of 10Gbps and with excellent values of quality factor.

El-Saeed et al. (2016) managed through a SOA-MZI to reach different logic gates: XOR, OR, NOR and XNOR with different number of bits for the binary input data signals at a transmission rate of 10Gbps with low input power. They analyzed the performance of the SOA-MZI for each logic gate by changing the number of bits in the two binary data signals.

In this paper, all-optical NOT logic gate is simulated, mainly based on Michelson interferometer (MI) with semiconductor optical amplifier (SOA) nonlinear phenomena cross gain modulation (XGM) and mechanism of co-propagating SOA-MI configuration along with non-linear property to design NOT gate using OptiSystem software. The remainder of this paper is organized as follows: in section 2 describes the theoretical foundation, in section 3 we present the SOA-MI design of NOT logic gate, in section 4 the results and discussions of the simulations and finally in section 5 the conclusions, acknowledgments and references.

2 THEORETICAL FOUNDATION

SOAs have been used over the years in wavelength conversion techniques through XGM, which consists of varying SOA gain as a function of input power, because as it increases there is a depletion of the optical carrier density and the amplification gain is reduced. As shown in Figure 1, the XGM causes an inversion of the shape of the input signal and acts as a wavelength converter by optical switching on the part of the amplifier (SON et al., 2007; AGGARWAL and SINGH, 2016).

Figure 1: Wavelength converter based on XGM in SOA

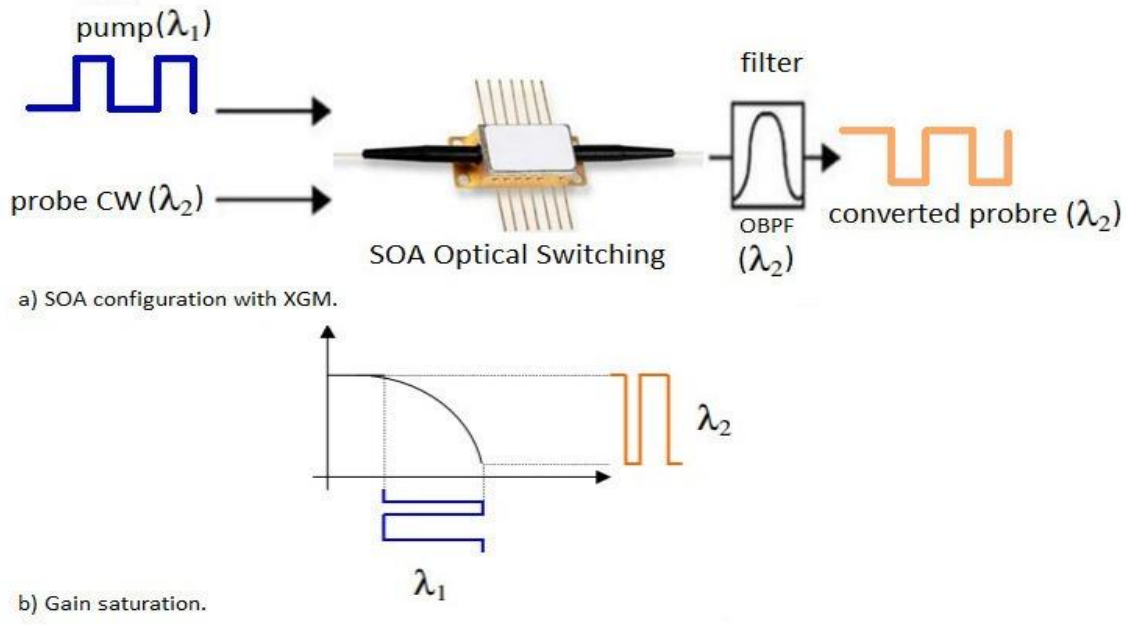

Source: Own authorship (2021).

The XGM effect occurs when a signal modulated in intensity in the wavelength λ_1 is injected into the SOA together with a signal CW in the wavelength λ_2 (EL-SAEED et al., 2016). A high-power input signal (Pump) is injected into the semiconductor optical amplifier to exhaust the maximum number of carriers (decrease density) present in the active SOA region, causing compression/variation of the amplifier gain due to depletion caused by stimulated emission in the presence of a high power source when the signal is amplified (OLIVEIRA, 2018).

Thus, if a lower power signal, for example, the Probe signal, is injected simultaneously with the Pump, being coupled to the SOA, the Probe will suffer attenuation due to the absorption of the carriers, and the pump gain increases. Gain modulation caused by input signal modulates the weak continuous wave (CW) signal in the output wavelength, thus increasing the distortion of the output signal. As a result of the change in carrier density, a change in the refractive index is also induced (AGGARWAL and SINGH, 2016).

If an optical pulse is present in the Pump signal, the SOA gain decreases and, therefore, the continuous Probe signal experiences low amplification. Otherwise, if there is no pulse of light at the Pump input signal, at λ_1, the gain of the device increases. This results in the continuous wave (CW) signal at λ_2 experiencing high amplification, thus, the pump input signal is inverted at the output (SILVEIRA, 2011).

From a certain point the current increase is no longer as efficient, due to the dependence of the internal gain with the input power. The internal gain g that occurs in the active SOA region is defined by (OLIVEIRA, 2018):

$$g(n) = \Gamma v_g g_m(n) = \Gamma v_g \alpha(n - n_0) \quad (1)$$

where α is the variation of the gain in relation to n, the differential gain; n is the density of carriers in the active region, and n_0 is the density of carriers in transparency, Γ is the confinement factor of the optical field in the active region, and v_g is the group velocity of the incident field.

Thus, when the incident power in the amplifier approaches the saturation power, the power by which the gain drops in half, the amplifier is no longer linear with the power, and the gain drops with an increase in power. Therefore, the total gain, G is defined by (CAVALCANTE, 2017; KUMAR, 2013).

$$G = \frac{G_0}{1 + \frac{P_{in}}{P_{sat,in}}} \quad (2)$$

where G_0 is the unsaturated gain, called the "small signal" gain, P_{in} is the input power and $P_{sat,in}$ is the input saturation power.

Optical passband filters (OBPF) are needed to filter the signal at the output of the converter device, which filters the wavelength λ_1 and lets pass λ_2, which was modulated in the conversion process. If the laser of the CW signal probe and the filter are tunable, then there is a tunable converter, otherwise the converter is called fixed (OLIVEIRA, 2018).

The Bragg grid (FBG) consists of periodic modulation / variation / disturbance in the refractive index of the fiber core, with properties of the reflection coefficient capable of reflecting (short period) or transmitting (long period) light as a function of the length of wave of the Bragg grating (λ_B) depending on the widening of the pulse, as well as its power, and is related to the spatial periodicity of the refractive index modulation (Λ) and

the effective refractive index of the core (n_{eff}) according to the equation (SOUSA et al., 2019):

$$\lambda_B = 2n_{eff}\Lambda \tag{3}$$

Figure 2: Operation Scheme of Fiber Bragg Grating.

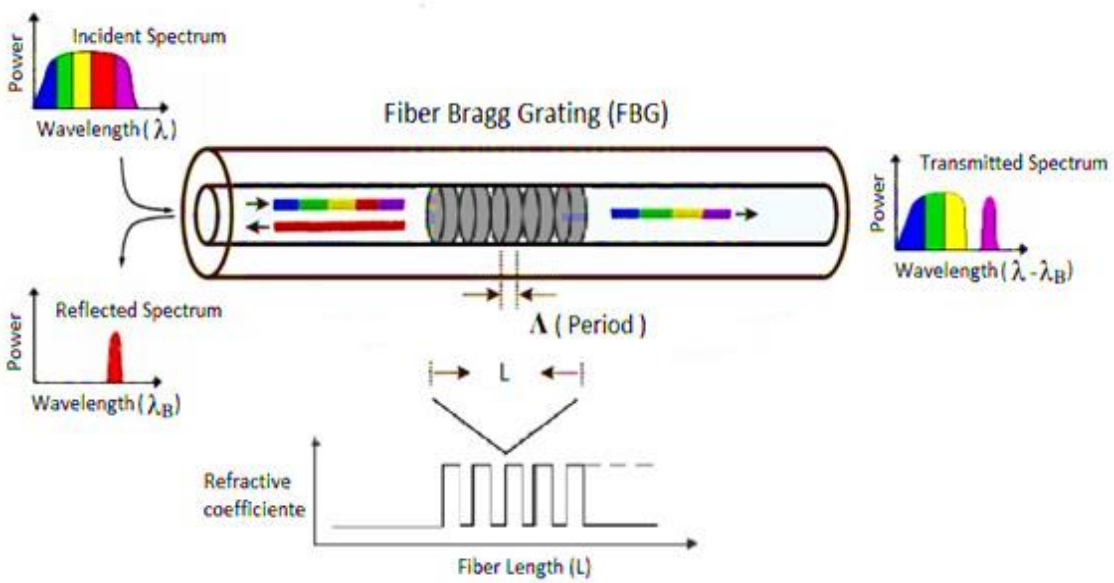

Source: Own authorship (2021).

Figure 2 represents an FBG being illuminated by a wide spectral band light source, in which a narrow band of this light spectrum centered on Bragg's wavelength will be reflected while the rest of the spectrum is transmitted. Therefore, FBG operates as a counter-directional energy coupler, and as a type of spectral reflector filter built inside an optical fiber capable of reflecting/selecting a range of wavelengths, remaining relatively transparent to the rest of the spectrum.

3 MATERIAL AND METHODS

In optical fibers the configuration of the Michelson interferometer can be obtained from the cascade association of two optical components: a directional coupler and 100% reflective linear Fiber Bragg Grating (FBG) [8].

The Boolean expression for NOT gate is $\boldsymbol{S = \overline{A}}$, where A is input signal and S is output. When the input A of NOT gate are “1” the output S is “0”. If the input is “0”, the output S is “1”. Block schematic is shown in Figure 3 and its truth table in Table 1. In the

NOT operation performed on the input data, the signal generated at a wavelength of λ_1 and a CW Laser at wavelength λ_2 injected as control beam, in this way, the result centered at λ_2 is the INVERT.

Figure 3: Block schematic of NOT gate based on SOA-MI

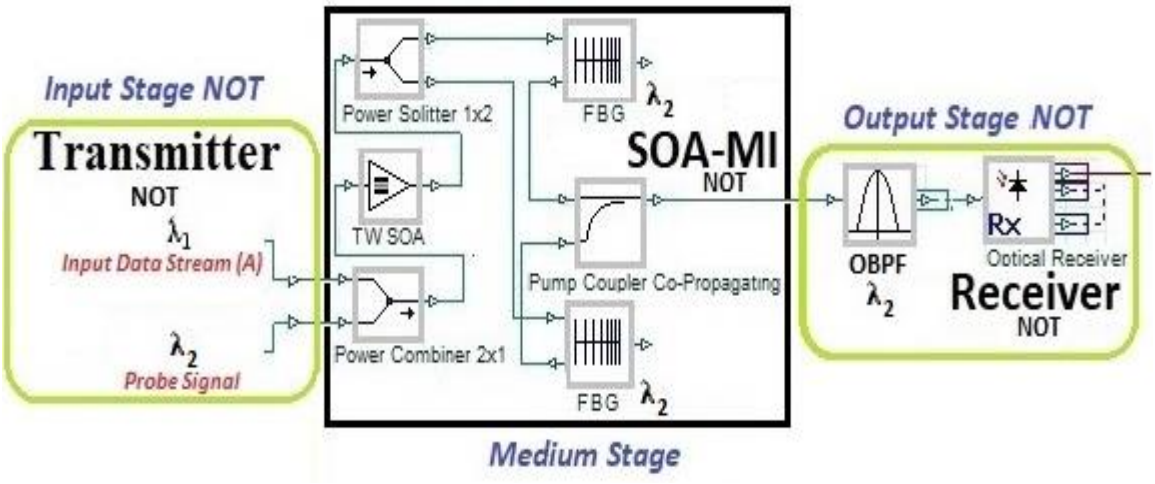

Source: Own authorship (2021).

Table 1: Truth table for NOT gate

Input A	Output $S = \overline{A}$	Symbol of NOT gate
0	1	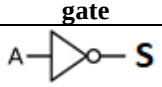
1	0	

Source: Own authorship (2021).

In the Figure 4 is shown the INVERT design, where the transmitter of NOT gate is formed of one input signal A generated from the Bit Sequence Generator with the Optical Gaussian Pulse generator at wavelength 1545nm with input power at 0.5mW, and combined with a Continuous Wave Laser (CW laser) of 1540nm with input power at 0.4mW, through a Power Combiner 2x1, at a transmission bit rate of 20Gbps.

The signal from port along with the control signal enters the SOA-MI, where are coupled by a Power Combiner 2x1 whose output propagate is amplified in the Traveling Wave (TW-SOA) with injection current range from 0.05 to 1.0 *A* and length of 0.0005 *m*, which in turn is connected to a Power Splitter 1x2 having both symmetrically identical FBGs with frequencies equal to those of the CW Laser (at 1540nm), where the output signals of the FBGs are again coupled through the Pump Coupler Co-Propagating, forming the SOA-MI of NOT gate.

The receiver of NOT gate consists of a Gaussian Optical Filter operates at 1540nm with a bandwidth of 40GHz, rejecting interferences and noise, and then is optically converted to electrical form through the Optical Receiver, with a cut-off frequency of 0.75 * bit rate Hz, and is delivered to a NRZ Pulse Generator.

Figure 4: Project of All-optical NOT logic gate with SOA-MI

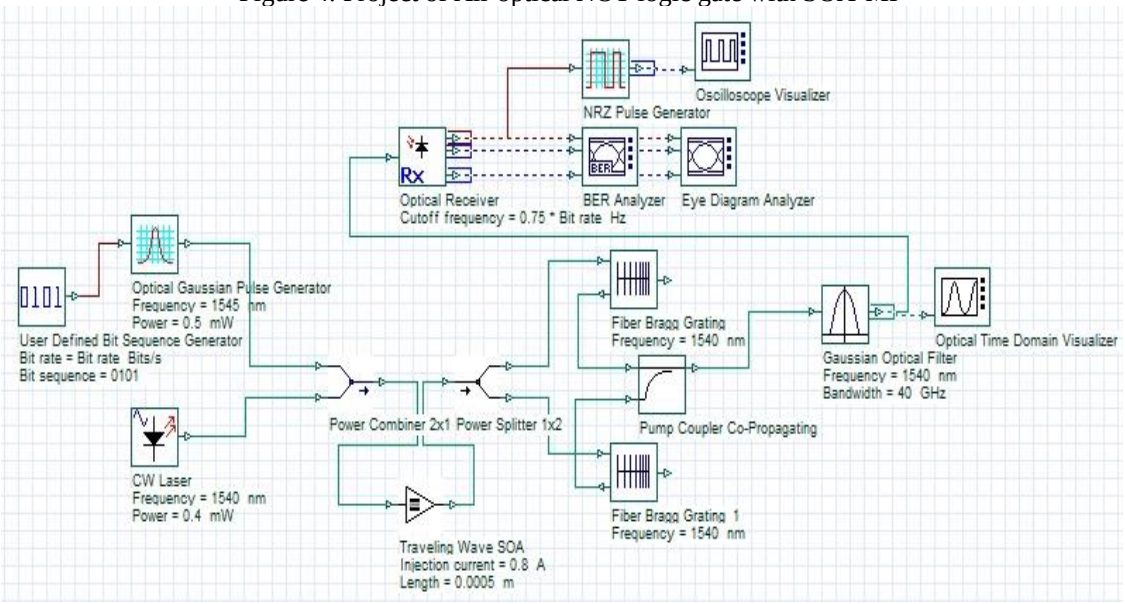

Source: Own authorship (2021).

The Table 2 shows the parameters of the SOA used in this project, where the injection current varied to find the best result of the Q-Factor with different numbers of bits in the input signal.

Table 2: Parameters used for SOA in simulations

SOA Parameters	Assigned Values
Injection current	$0{,}05 - 1.0\ A$
Length	$500\ \mu m$
Width	$3\ \mu m$
Height	$80\ nm$
Optical confinement fator	0,3
Differential gain	$2{,}78\ \times 10^{-20}\ m^2$
Carrier density at transparency	$1{,}4\ \times 10^{24}\ m^{-3}$
Linewidth enhancement factor	5
Recombination coefficient of surface and defect	$1{,}43\ \times 10^{8}\ s^{-1}$
Recombination coefficient of radiative	$1 \times 10^{-16}\ m^3\ \cdot s^{-1}$
Recombination coefficient Auger	$3\ \times 10^{-41}\ m^6\ \cdot s^{-1}$
Initial carrier density	$3\ \times 10^{24}\ m^{-3}$

Source: Own authorship (2021).

The performance analysis of the Michelson interferometer we used the max. Q-factor and min. BER. In this sense the Q-factor is defined by (SOUSA et al., 2020):

$$Q_{factor} = \frac{I_1 - I_0}{\sigma_1 + \sigma_0} \quad (4)$$

where the eye range is the difference between the average value of '1' level and '0' level, the signal noise RMS is the sum of '1' noise RMS σ_1 and '0' noise RMS σ_0. I_1 and I_0 are the currents generated in the receiver for each bit.

The BER is regarded as the number of wrong bits divided by the total number of bits transferred in a communication system over a time interval (Agrawal 2012; Zhang and Zhao 2018;).

$$BER = \frac{1}{2} erfc\left(\frac{Q}{\sqrt{2}}\right) \approx \frac{\exp(-Q^2/2)}{Q\sqrt{2\pi}} \quad (5)$$

, where is the $erfc(x) = \frac{2}{\sqrt{\pi}} \int_0^x e^{-y^2} dy$

complementary error function.

4 RESULTS AND DISCUSSION

The Table 3 shows the different bit numbers used for the 4, 8, 16 and 32-Bit input information signals and the outputs of the NOT logic gate.

Table 3: The different number of bit for NOT operation

	Number of Bit			
Signal	**4-Bit**	**8-Bit**	**16-Bit**	**32-Bit**
Input A	0101	01011111	0101111111011111	11111111111100110101011110110110
Output S	1010	10100000	1010000000100000	00000000000011001010100001001001

Source: Own authorship (2021).

The design has an injection current range in the TWA SOA to find the best result and with the aid of the Eye diagram, the Max. Q-Factor, Min. BER and OSNR are also listed in Table 4 to analyze the performance of the NOT gate for different binary input. The Figure 3 shows the relationship between Q-factor and Injection Current, where a given number of bit input signal of Port A has its results in the injection current range from 0.05 to 1.0 A of TWA SOA.

Table 4: Analysis of Results of 40 GHz for 4, 8, 16 and 32-Bit at 20 Gb/s

	Number of Bit			
Parameters	**4-Bit**	**8-Bit**	**16-Bit**	**32-Bit**
Max. Q-Factor	33.2838	27.5154	26.1326	24.1900
Min. BER	3.30056e-243	4.13969e-167	5.4715e-151	8.90981e-130
Eye Height	0.0846453	0.0677146	0.105157	0.0613351

Source: Own authorship (2021).

It was observed in figure 5 that the injection current of 0.05 and 0.1A obtained Q-factor equal to 0 (zero) showing that it should be used from 0.15A, the default value being suggested by the OptiSystem software. Among the bit numbers, the 4-bits sequence was the one with the best values, with max. Q-Factor equal to 3.2, min. BER equal to 0.5e-003, because the larger the number of bits, the smaller the Q-factor. The following topics show the results for each input bit sequence. For a better visualization of the results, the images were organized according to the bit sequence quantity for the bandwidth of the Gaussian Optical Filter of 40GHz at 20Gbps.

Figure 5: Results of Max. Q-Factor x Injection Current range for NOT gate

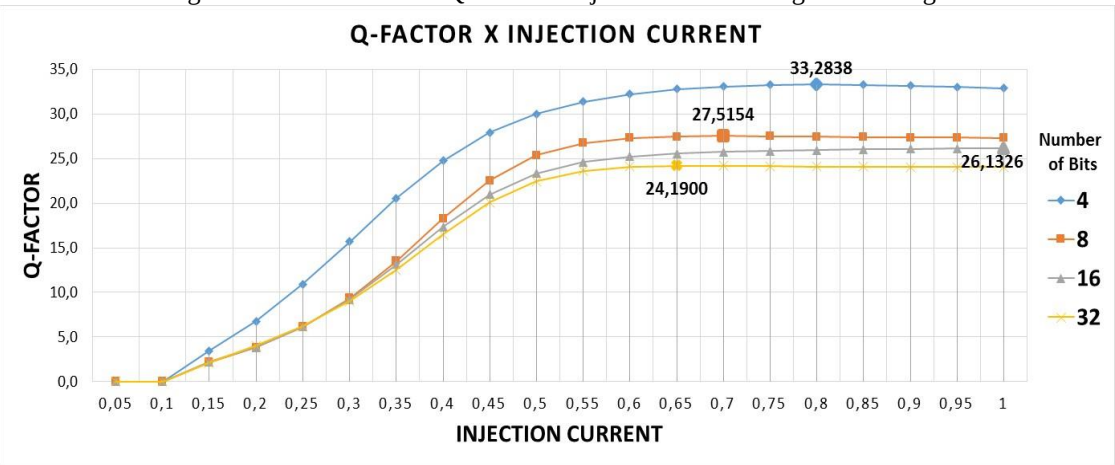

Source: Own authorship (2021).

A. The results for 4-bits input signal

It obtained the better result for the Max. Q-Factor equal to 33.2838 and Min. BER equal to 3.30056e-243 with injection current equal to 0.8A in the TW-SOA with input signal 0101, in the transfer from 4-bit at 20Gbps bit rate. In figure 6 we find this result. The eye diagram and the Q Factor are shown in Figure 6(a). The output of the NOT gate 1010 is shown in Figure 6(b), in oscilloscope.

Figure 6: (a) Eye Diagram and Max. Q-Factor and (b) signal result for the NOT gate with **4-bits** input and injection current of **0.8 A** at 20 Gb/s

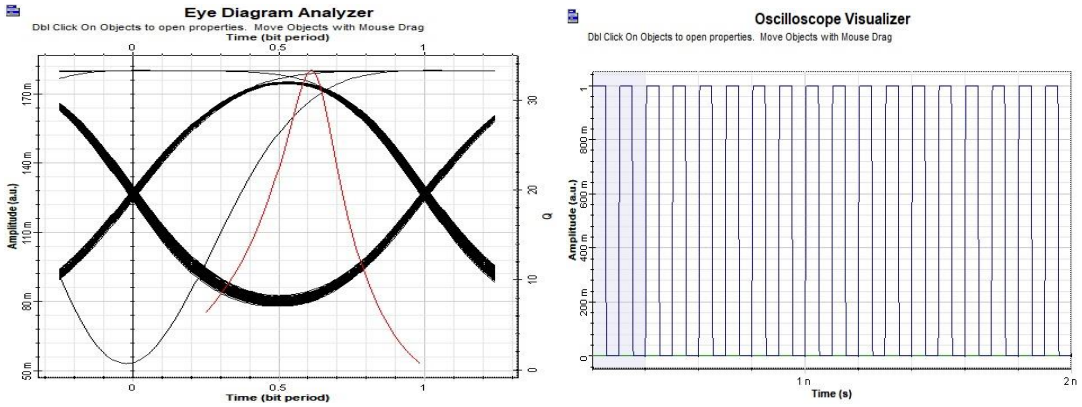

Source: Own authorship (2021).

B. The results for 8-bits input signal

The input signal 01011111, in the transfer from 8-bit at 20Gbps bit rate with injection current equal to 0.7 *A* in the TW-SOA, it obtained the better result for the Max. Q-Factor equal to 27,5154 and Min. BER equal to 4.13969e-167. The eye diagram with the Q Factor are shown in Figure 6(a) and the output of the NOT gate 10100000 is shown in Figure 6(b).

Figure 6: (a) Eye Diagram and Max. Q-Factor and (b) signal result for the NOT gate with **8-bits** input and injection current of **0.7 A** at 20 Gb/s

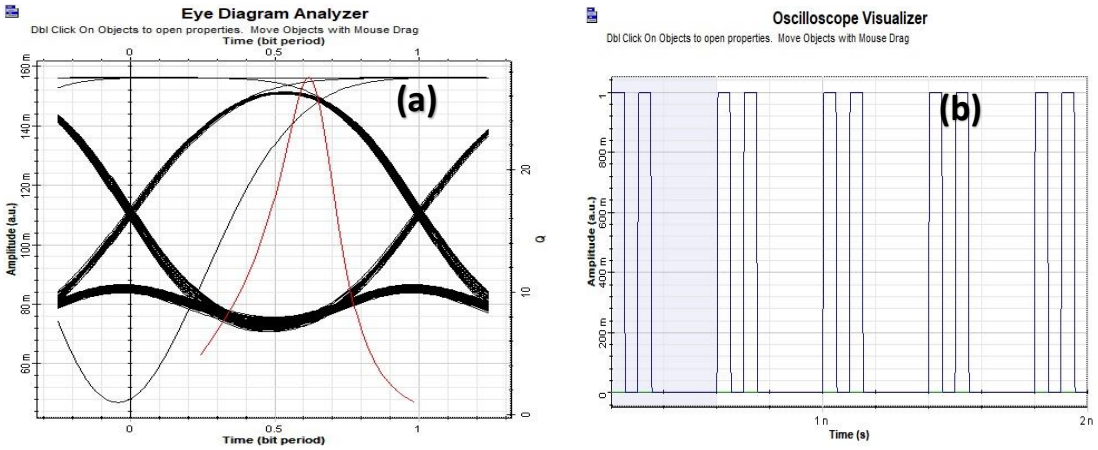

Source: Own authorship (2021).

C. The results for 16-bits input signal

The eye diagram with the Q Factor are shown in Figure 7(a) and the output of the NOT gate 1010000000100000 is shown in Figure 7(b) in oscilloscope with input signal

0101111111011111, in the transfer from 16-bit at 20Gbps bit rate, it obtained the better result Max. Q-Factor equal to 26.1326 and Min. BER equal to 5.4715e-151 with injection current equal to 1.0 *A* in the TW-SOA.

Figure 7: (a) Eye Diagram and Max. Q-Factor and (b) signal result for the NOT gate with **16-bits** input and injection current of **1.0 A** at 20 Gb/s

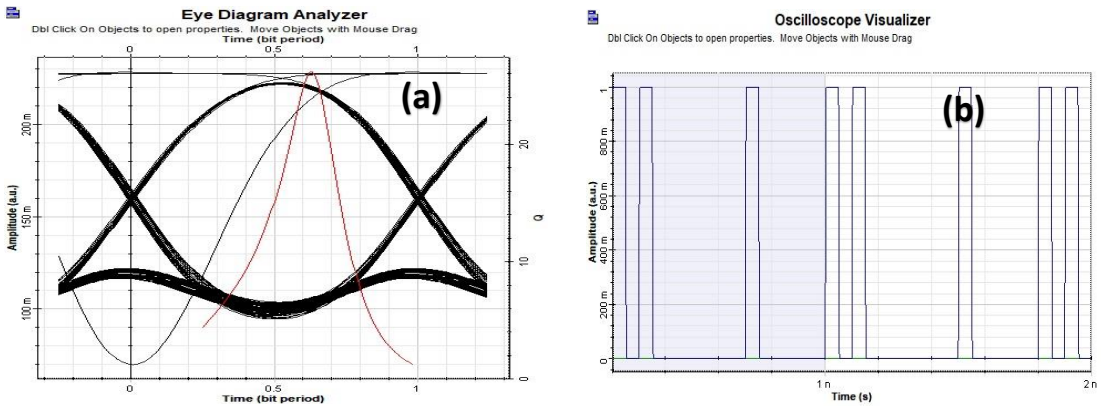

Source: Own authorship (2021).

D. The results for 32-bits input signal

In Figure 7 (a) shown the Eye Diagram with the better result Max. Q-Factor equal to 24.1900 and in Figure 7 (b) shown the output of the NOT gate 00000000000011001010100001001001 with input signal 11111111111100110101011110110110 in the transfer from 32-bit at 20Gbps bit rate with injection current equal to 0.65 A in the TW-SOA and it obtained the Min. BER equal to 8.90981e-130.

Figure 7: (a) Eye Diagram and Max. Q-Factor and (b) signal result for the NOT gate with **32-bits** input and injection current of **0.65 A** at 20 Gb/s

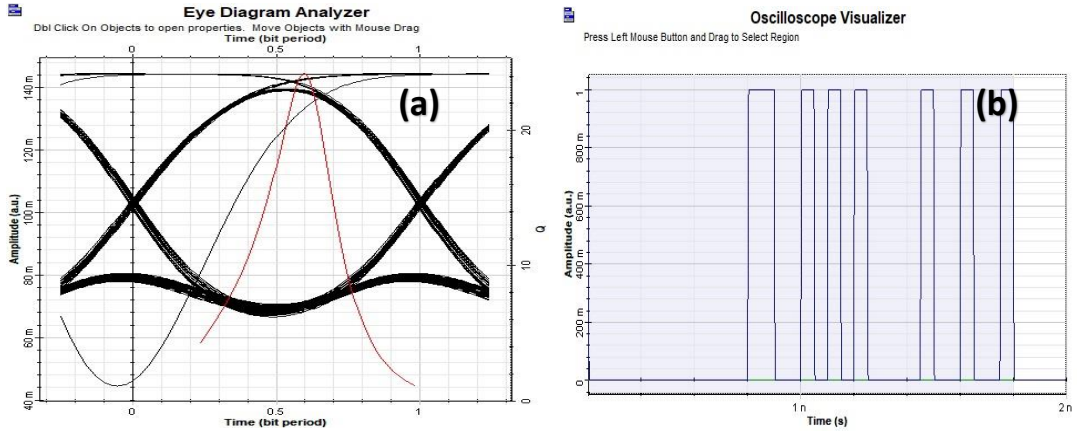

5 CONCLUSION

The All-optical NOT logic gate, have been simulated at 20 Gb/s using co-propagating and effect non-linear XGM of SOA. The obtained SOA-MI structure with results ensure good performance of the proposed design, using different bit numbers (4, 8, 16 and 32-bits) in the input signal, with the best quality factor (Q-factor) to optimum injection current of TW-SOA. In short, it is worth mentioning that several logic functions, such as AND, OR and NOR have already been carried out using the cross-gain modulation effect in SOAs in fiber optic communication systems with FBG and OBPF for different transmission rates. This has contributed to the creation and implementation of fiber optic communication systems of the future.

ACKNOWLEDGMENT

This study was financed in part by the Coordenação de Aperfeiçoamento de Pessoal de Nível Superior – Brasil (CAPES) – Finance Code 001.

The Federal Institute of Pará (IFPA), the Postgraduate Program in Electrical Engineering of the Federal University of Pará, Belém – Brazil and the Pró-Reitoria de Pesquisa e Pós-Graduação (PROPEP) da Universidade Federal do Pará (UFPA), Belém – Brasil.

REFERENCES

AGGARWAL, Kanika; SINGH, Hardeep Guide. Implementation of Optical Logic Unit Based on Nonlinear Properties of Semiconductor Optical Amplifiers. Department of Electronics & Communication Engineering – Thapar University, Patiala. 2016. Disponível em: http://117.203.246.91:8080/jspui/bitstream/10266/4062/4/4062.pdf. Acesso em: 10 jan. 2021.

ARCHANA, K.; MANOHARI, R.; PRINCE, S. Performance Analysis of Different Designs of All-optical D Flip Flop. **International Journal of Engineering and Technology**, v. 7, n. 2.8, p. 578-582, 2018. Disponível em: https://www.researchgate.net/publication/325117542_Performance_analysis_of_different_designs_of_all-optical_D_flip_flop. Acesso em: 15 jan. 2021.

CAVALCANTE, Daniel do Nascimento e Sá. Obtenção Experimental de Portas Lógicas com Interferômetro de Mach-Zehnder e SOA. Fortaleza: IFCE, 2017. Disponível em: http://biblioteca.ifce.edu.br/asp/download.asp?codigo=1551&tipo_midia=2&iIndexSrv=1&iUsuario=0&obra=63367&tipo=1&iBanner=0&iIdioma=0. Acesso em: 20 jan. 2021.

DUARTE, Camille Toscano et al. Método da Regressão Linear Múltipla Aplicado na Calibração de Sensores Inerciais. **Brazilian Journal of Development**, v. 6, n. 10, p. 75363-75371, 2020. Disponível em: https://www.brazilianjournals.com/index.php/BRJD/article/view/17819. Acesso em: 22 jan. 2021.

EL-SAEED, E. M., ABD EL-AZIZ, A., FAYED, H. A., & ALY, M. H. Optical Logic Gates Based on Semiconductor Optical Amplifier Mach–Zehnder Interferometer: Design and Simulation. **Optical Engineering**, v. 55, n. 2, p. 025104, 2016. Disponível em: https://www.researchgate.net/publication/293822143_Optical_logic_gates_based_on_semiconductor_optical_amplifier_Mach-Zehnder_interferometer_Design_and_simulation. Acesso em: 10 fev. 2021.

KUMAR, Ajay; KUMAR, Santosh; RAGHUWANSHI, S. K. Implementation of All-Optical Logic Gate Using SOA-MZI Structures. **STM Journals**, v. 3, n. 3, p. 13-21, 2013. Disponível em: http://engineeringjournals.stmjournals.in/index.php/TOEOC/article/view/1901. Acesso em: 10 fev. 2021.

MALHOTRA, N.; ANAND, S.; RAGHAV, P. K. Simulation of logic gates for digital optical networks using SOA. **Int J Sci Eng Res**, v. 5, p. 427-35, 2014. Disponível em: https://www.ijser.org/onlineResearchPaperViewer.aspx?Simulation-of-logic-gates-for-Digital-optical-Networks-using-SOA.pdf. Acesso em: 15 fev. 2021.

MAZLAN, Intan Zubaidah; WAHID, Mohamad Halim Abd; HASSAN, Ahmad Fariz; AZIDIN, Mohd. Azarulsani Md. and ISA, Noor Faridah Mat. Cross Gain Modulation (XGM) Based on Wavelength Conversion Using Semiconductor Optical Amplifier and Filter. **Int. J. Microw. Opt. Technol**, v. 9, n. 1, p. 115-118, 2014. Disponível em: https://www.semanticscholar.org/paper/Cross-Gain-Modulation-(XGM)-Based-On-

Wavelength-and-Mazlan-Halim/4b83a32d236438fce705ef38ff34e36e0c2b22c6. Acesso em: 25 fev. 2021.

MUKHERJEE, K. and RAJA, A.; MAJI, K. All-optical logic gate NAND Using Semiconductor Optical Amplifiers with Simulation. **Journal of Optics**, v. 48, n. 3, p. 357-364, 2019. Disponível em: https://link.springer.com/article/10.1007/s12596-019-00555-9. Acesso em: 25 fev. 2021.

OLIVEIRA, Jackson Moreira. Portas Lógicas Totalmente Ópticas Baseado em Interferômetro de Michelson com Amplificador Óptico Semicondutor. Dissertação de Mestrado. **Universidade Federal do Pará, (Brasil)**, 2018. Disponível em: http://repositorio.ufpa.br:8080/jspui/handle/2011/10275. Acesso em: 10 març. 2021.

OLIVEIRA, Jackson Moreira et al. New Design of All-Optical Logic Universal NAND Gate Formed by NOT (A AND B) Gates Using Michelson Interferometer Based on Semiconductor Optical Amplifier. **Journal of Computational and Theoretical Nanoscience**, v. 16, n. 7, p. 2712-2719, 2019. Disponível em: https://www.ingentaconnect.com/content/asp/jctn/2019/00000016/00000007/art00009;jsessionid=2gifv5jfg05j.x-ic-live-02. Acesso em: 10 març. 2021.

SINGH, Supreet Kumar; TIWARI, Nidhish; RAJCHANDANI, Uma. Implementation of Optical Logic Gates (Ex-OR AND and NOR) using SOA-MZI Structure. **The International Journal of Science and Technoledge**, v. 2, n. 7, p. 158, 2014. Disponível em: https://search.proquest.com/openview/fb91d6e080504136f5bc1eae484fdfdc/1.pdf?pq-origsite=gscholar&cbl=2035011. Acesso em: 10 març. 2021.

SON, C. W.; KIM, S. H.; JHON, Y. M.; BYUN, Y. T., LEE, S., WOO, D. H. and YOON, T. H. Realization of All-Optical XOR, NOR, and NAND Gates in Single Format by Using Semiconductor Optical Amplifiers. **Japanese journal of applied physics**, v. 46, n. 1R, p. 232, 2007. Disponível em: https://iopscience.iop.org/article/10.1143/JJAP.46.232/meta. Acesso em: 10 març. 2021.

SOUSA, Fabio Barros de; SOUSA, Fiterlinge Martins de; OLIVEIRA, Jorge Everaldo de; OLIVEIRA, Lelis Araujo de; LUZ, Fabricio Pinho da; OLIVEIRA, Jackson Moreira; COSTA, Marcio Benedito Caldas; PASCHOAL JUNIOR, Waldomiro; SILVA JUNIOR, Carlos Alberto Brito da and Costa, Marcos Benedito Caldas. Numerical Analysis of the Hybrid Photonic Crystal Fiber and Single Mode Fiber/Fiber Bragg Grating Sensor for Simultaneous Measurement of Temperature and Strain. **Journal of Computational and Theoretical Nanoscience**, v. 16, n. 2, p. 329-334, 2019. Disponível em: https://www.ingentaconnect.com/contentone/asp/jctn/2019/00000016/00000002/art00001. Acesso em: 10 març. 2021.

SOUSA, Fabio Barros de, Sousa, Fiterlinge Martins de, Oliveira, Jorge Everaldo de, Paschoal, Waldomiro and Costa, Marcos Benedito Caldas. Numerical analysis of the performance of a Mach–Zehnder interferometer based on acousto-optic filter for signal regeneration. **Optical and Quantum Electronics**, v. 52, p. 1-12, 2020. Disponível em: https://link.springer.com/article/10.1007%2Fs11082-020-02389-3. Acesso em: 10 març. 2021.

VINOTHINI, M.; SHANMUGAPRIYA, P; MARGARAT, M. Design and Simulation of All-Optical logic Gates Using SOA-MZI. **Journal for Advanced Research in Applied Sciences**, p.181-187, 2018. Disponível em: http://www.iaetsdjaras.org/gallery/22-april.pdf. Acesso em: 10 març. 2021.

SILVEIRA, Tiago Gomes da. All-Optical Processing Systems Based on Semiconductor Optical Amplifiers. Tese de Doutorado. **Universidade de Aveiro (Portugal)**, 2011. Disponível em: https://ria.ua.pt/handle/10773/7028?locale=pt_PT. Acesso em: 10 març. 2021.